ChemPubSoc Europe

DOI: 10.1002/cphc.201402613

Electronic Properties of Transition-Metal-Decorated Silicene

Youngbin Lee, Kyung-Han Yun, Sung Beom Cho, and Yong-Chae Chung*[a]

The electronic properties of 3d transition metal (TM)-decorated silicene were investigated by using density functional calculations in an attempt to replace graphene in electronic applications, owing to its better compatibility with Si-based technology. Among the ten types of TM-doped silicene (TM–silicene) studied, Ti-, Ni-, and Zn-doped silicene became semiconductors, whereas Co and Cu doping changed the substrate to a half-metallic material. Interestingly, in cases of Ti- and Cu-doped silicene, the measured band gaps turned out to be significantly larger than the previously reported band gap in silicene. The observed band-gap openings at the Fermi level were induced by breaking the sublattice symmetry caused by two structural changes, that is, the Jahn–Teller distortion and protrusion of the TM atom. The present calculation of the band gap in TM–silicene suggests useful guidance for future experiments to fabricate various silicene-based applications such as a field-effect transistor, single-spin electron source, and nonvolatile magnetic random-access memory.

1. Introduction

Recently, silicene has been intensively researched for manufacturing nanoelectronic devices as a promising alternative to graphene.[1–3] Although graphene has remarkable characteristics such as a structural simplicity and high electronic conductivity,[4–5] it has a compatibility problem with currently dominant silicon-based electronic devices because it is a carbon allotrope. To be better compatible with the silicon-based technology, silicene has been attracting considerable attention, as silicene is composed of a silicon (Si) atom with the similar benefits of graphene mentioned above.[6–9] Silicene has a two-dimensional honeycomb structure with buckling by the partial involvement of a $3p_z$ orbital in the Si–Si bond,[1–2,9–11] and it has recently been experimentally synthesized on Ag (111), Ir (111), and ZnB_2.[3,12–17] In addition to the advantage of compatibility mentioned above, another superior characteristic of silicene as an electronic device compared to graphene is that silicene is a strong candidate for the quantum spin hall effect, because silicene has a larger band gap than graphene at low temperatures.[7,18–19] Thus, studies of the electronic properties of silicene are of potential importance in diverse fields such as quantum electronics, spintronics, and optoelectronics.[20–24]

To apply silicene with useful electronic features, especially those associated with the band gap, to nanoelectronic devices, it is necessary to examine the band-gap opening in silicene. A number of methods such as impurity doping, defect formation, and applying an electric field have been used to modulate the band gap.[25–34] If a gap induced by these means has semiconducting or half-metallic characteristics at a range including the Fermi level (E_F), a system with this band gap can be applicable to practical areas, such as field-effect transistors (FETs), single-spin electron sources, and nonvolatile magnetic random access memory (MRAM).[20–24] Consequently, many ways to open a band gap for these devices have been attempted by using silicene.[18,34–41]

In the present paper, detailed studies of the effect of 3d transition metal (TM) atom doping on the band-gap opening of silicene were performed by using first-principles density functional theory (DFT) calculations. Here, 3d TM atoms (from Sc to Zn in the Periodic Table) were used, as it is thought that different properties will be introduced because of the partially occupied 3d orbital.[41] Also, the substitution of 3d TM atoms in silicene has the purpose of more finely dispersing the TM atom than in cases of adsorption.[1,41] This first exploration of 3d TM doping on silicene will facilitate a potential method for band-gap opening at E_F.

Computational Methods

DFT calculations were conducted by using the Vienna ab-initio simulation package (VASP).[42–44] All calculations were carried out under the Perdew–Burke–Ernzerhof (PBE)[45] generalized gradient approximation (GGA) with a projector augmented wave (PAW) pseudopotential method[46] for the exchange-correlation potential. A plane wave basis was set with a cutoff energy of 500 eV, and a 6×6×1 Gamma Monkhost-Pack[47] k-point grid was used to sample the Brillouin zone. A Gaussian broadening scheme was used with a width of 0.05 eV, and a 12×12×1 Gamma Monkhost-Pack k-point mesh was used to calculate the density of states (DOS). The atomic positions were relaxed by using the conjugate gradient method and optimized until the maximum force on any atom became less than 0.02 eV Å^{-1}. The criterion for energy convergence was a 10^{-5} eV cell^{-1}.

[a] Y. Lee, K.-H. Yun, S. B. Cho, Prof. Y.-C. Chung
Department of Materials Science and Engineering
Hanyang University, Seoul, 133-791 (Korea)
E-mail: yongchae@hanyang.ac.kr

Supporting Information for this article is available on the WWW under http://dx.doi.org/10.1002/cphc.201402613.

To simulate TM-doped silicene (TM–silicene), the system was modeled with a vacuum spacing of 20 Å. The unit cell of the system was decided by using a strict energy-convergence test. From this result, a lattice parameter at 3.868 Å was used; the configuration of the pristine silicene supercell is shown in Figure 1. As mentioned

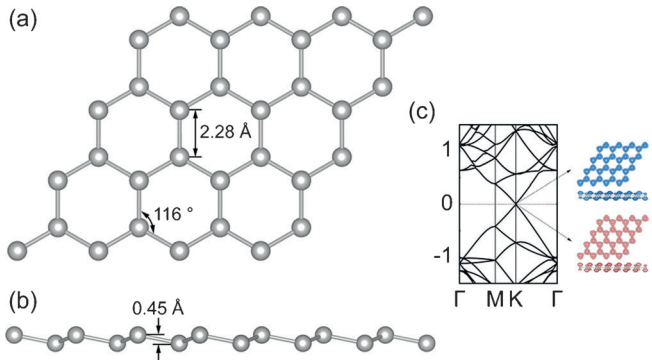

Figure 1. Geometry of the pristine silicene: a) top view and b) side view. c) Band structure of pristine silicene, with insets representing the charge density for the topmost valence band and the lowest conduction band in the vicinity of the *K* point.

previously, silicene is a two-dimensional honeycomb structure with buckling in the partial sp^3 hybridization of the Si–Si bond.[1–2,9–11] The length of the Si–Si bond in silicene (d_{Si-Si}) is 2.28 Å, and the buckled height (h_{Si}) is 0.45 Å. From this buckling, two equivalent Si sublattices are introduced, and these two sublattices have symmetry. When a TM atom substitutes a Si atom in this system, the band-gap properties are strongly dependent on the supercell size, which is related to the doping concentration and substitution site of the TM atom.[34] For example, if TM–silicene has a supercell size satisfying Kekule's rule, different results for a band-gap opening may occur.[34] However, because the present work focuses on the effect of each type of 3d TM on the electronic structure of silicene when single-doped TM atom influences silicene, the modeled system was fixed as a 4×4 supercell for the efficiency and rationality of the calculations. The length of 4×4 supercell corresponds to 15.472 Å, which is clearly over 10 Å that has been generally selected to remove the interactions between the nearest TM atoms.[48] In this study, the concentration of the TM atom was about 3.2 at% in TM–silicene. To ensure that the structures used in the present paper are in the most stable states, the relaxations of TM–silicene were repeated by using various different initial heights of the TM atom.

2. Results and Discussion

Prior to confirming the band-gap opening in silicene by TM doping, the structural stability of TM–silicene was studied. The geometric stability can be considered as the same as the maintenance of the well-dispersed state of the TM atoms, and this is important for uniform properties in the entire TM–silicene substrate. Here, for the stability of the TM–silicene system, the binding energy (E_b) between the TM atom and silicene was calculated by using Equation (1):

$$E_b = E_{TM} + E_{SVS} - E_{TM-Sil} \quad (1)$$

where E_{TM}, E_{SVS}, and E_{TM-Sil} represent the energies of an isolated TM atom, silicene with a single vacancy, and the total system of TM–silicene, respectively. These obtained E_b values are larger than the cohesive energies of each TM bulk energy (E_c) in all cases of TM doping (Figure 2). These results mean that the TM atoms do not form a cluster and can be preserved in a well-distributed condition on the silicene substrate. In addition, by comparing these values with the results of a previous study on

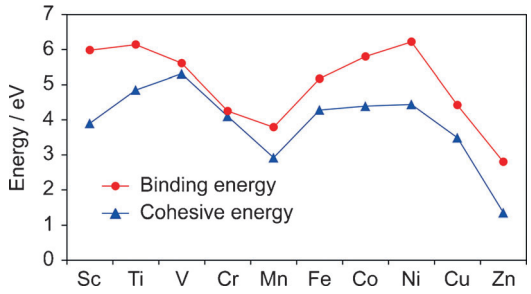

Figure 2. Silicene binding energy and cohesive energy in the bulk state, according to TM atom. The red and blue lines represent the binding and cohesive energy, respectively.

the adsorption of TM atoms on silicene, it is supposed that the TM–silicene system can be more finely controlled than a TM-adsorbed silicene system.[1] Therefore, this retention of a good dispersion of the TM atoms on silicene indicates that TM–silicene is a stable system in itself, which is more appropriate for applications compared to other systems comprised of the TM atom and silicene in terms of structural stability.

To ascertain the existence of a band-gap opening in TM–silicene, which is a geometrically stable system, the band structures of TM–silicene were investigated. In general, various effects such as metal adsorption or applying an electric field to silicene led to a gap opening in the Dirac cone.[18,34,40] Among these gaps, a gap opening at the E_F is more notable for practical nanoelectronic devices than a gap that is opened at other energy levels, because the flow of electrons can be tunable by the size of the band gap at the E_F. From the calculation, although Sc, V, Cr, Mn, and Fe doping induce a gap opening, these gaps do not include E_F, as shown in Figure S1. Therefore, these substrates are still metallic, and there is no band gap. On the other hand, because Ti-, Co-, Ni-, Cu-, and Zn-doped silicene have a band-gap opening at E_F, which is more important from an engineering standpoint, these five systems were studied in more detail.

The band structures of TM–silicene, in which a band-gap opening is introduced at E_F, are presented in Figure 3. In these band structures, the Dirac cone in pristine silicene disappears. This is because the orbitals of the TM atom make a considerable contribution to the energy level through hybridization between the TM atom and the silicene (Figure 3). From this variation in the electronic structure by TM doping, a semimetallic silicene with a small direct band gap changes to a substrate with one of two significant band gaps for diverse devices. Ti-, Ni-, and Zn-doped silicene materials become semiconductors,

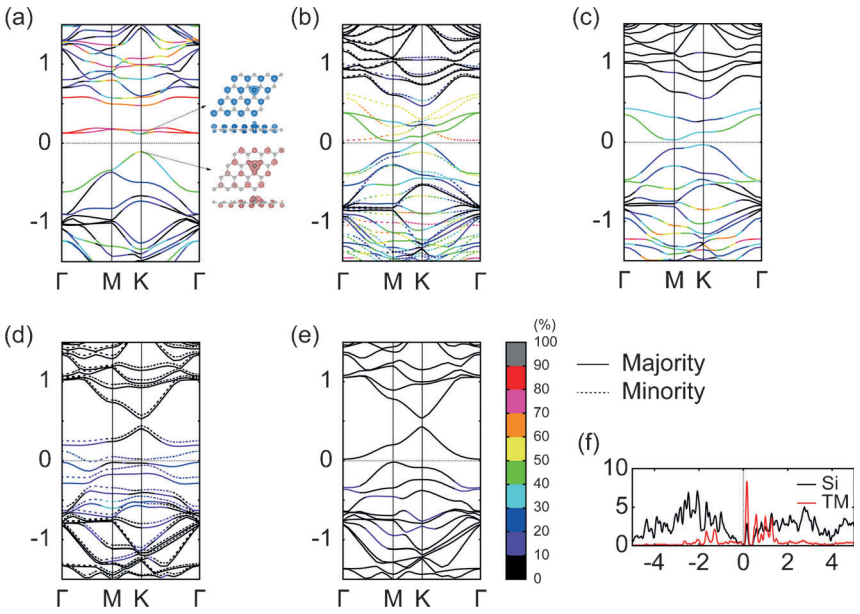

Figure 3. Electronic structures of TM–silicene, which has a band gap at the E_F. The band structures of a) Ti-, b) Co-, c) Ni-, d) Cu-, and e) Zn-doped silicene are presented. The solid and the dotted lines represent the majority-spin and minority-spin in Co- and Cu-doped silicene, respectively. The percentages of the contributions of the TM atom to the energy level are marked in different colors, and the Fermi level is set to zero. f) The partial density of states (PDOS) of Ti–silicene is indicated as the representative TM–silicene. The black and red lines represent the PDOS of the silicene and the TM atom, respectively. Insets in (a) represent the charge density for the topmost valence band and the lowest conduction band in the vicinity of the *K* point.

As mentioned in the Computational Methods section, silicene has two symmetric Si sublattices. From the two symmetric sublattices, the electrons in silicene behave as massless Dirac Fermions. This phenomenon can be verified by linear dispersion at E_F, as shown in Figure 1.[7–8,30,49] Owing to this obvious fact that the electronic features are significantly correlated with the geometric properties in silicene, the most stable configurations of TM–silicene are presented in Figure 4 to clarify the origin of the band-gap openings by TM doping in silicene. When the TM atom is substituted in silicene, Ti and Zn atoms are located at the center of the three nearest Si atoms (Figure 4a). On the other hand, the three Si neighbors around the Co, Ni, and Cu atoms are asymmetrically displaced, and the substrates are locally

which have a band-gap opening in both spin channels. On the other hand, Co and Cu doping alter silicene to a half-metallic material, as one spin channel becomes metallic, whereas the other has a semiconducting band gap caused by spin polarization in the substrate. The characteristics of these band-gap openings are listed in Table 1. From this information, it is anticipated that Ti- and Cu-doped silicene are more advantageous among the five TM–silicene materials, owing to the relatively large direct band gap. For example, Ti-doped silicene has a direct band gap of 221 meV at the *K* point, and this value is larger than that created when an external vertical electric field of 1.03 V Å^{-1} is applied to silicene ($E_g = 160$ meV).[40] Importantly, these band-gap openings in TM–silicene suggest a promising route, using silicene-based materials for the design of devices such as FET, nonvolatile MRAM, and a single-spin electron source.

Table 1. Band-gap properties of five types of TM–silicene that have a band gap at E_F. The properties listed are the point of the valence-band maximum (VBM), point of the conduction-band minimum (CBM), band-gap type, and band-gap size (E_g). Co- and Cu-doped silicene have a band gap in only one spin channel, and this spin channel is represented in parentheses. The direct and indirect band gaps are denoted by D and I in the band gap type, respectively.

	VBM	CBM	Band-gap type	E_g [meV]
Ti	*K*	*K*	D	221
Co (minority)	*K*	*Γ*	I	155
Ni	*K*	*M*	I	61
Cu (majority)	*Γ*	*Γ*	D	219
Zn	*M*	*Γ*	I	35

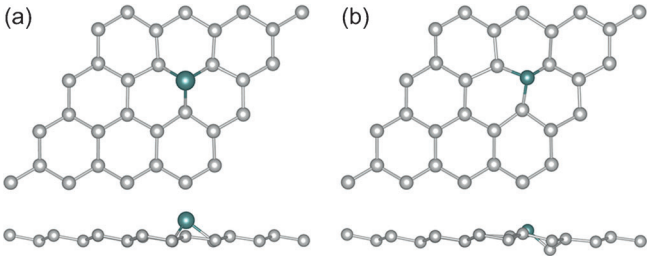

Figure 4. The most stable configurations of TM–silicene through a) Ti and Zn doping and b) Co, Ni, and Cu doping.

distorted (Figure 4b). These surrounding asymmetric geometries of the TM atom are caused by the Jahn–Teller effect. Previous works have reported that the Jahn–Teller distortion is induced by a nonsymmetric vibration derived from a vibronic coupling between the unoccupied molecular orbitals and occupied molecular orbitals, which are the nondegenerate electronic states of proper symmetry;[50–52] similar phenomena have been also observed in cases of adsorption and substitution of the TM atom on silicene and graphene, respectively.[53–54] From this perspective, it can be considered that the relatively small band gap of Co-, Ni-, and Cu-doped silicene introduces the Jahn–Teller distortion through the vibronic coupling between the CBM and VBM, and this effect is confirmed by the existence of the two values in the distances between the TM atom and the three Si neighbors (d_{TM-Si}), as listed in Table 2. Another noticeable change in the geometry of TM–silicene is that the doped TM atom protrudes out of two sublattices (Table 2). As

Table 2. Geometric properties and charge transfer for the five types of TM–silicene that have a band gap at E_F. The properties listed are the average height of a TM atom from the three nearest Si atoms (h_{TM}), distance between the TM atom and the Si neighbors (d_{TM-Si}), and the charge transfer by the Bader charge (Δq).[55]

	Ti	Co	Ni	Cu	Zn
h_{TM} [Å]	1.29	0.78	0.46	0.24	0.11
d_{TM-Si} [Å]	2.44	2.20	2.19	2.24	2.32
		2.23	2.24	2.26	
Δq	−1.01	0.38	0.42	0.18	−0.10

mentioned above, from the relation between the geometric and electronic structure, it can be expected that these structural characteristics, such as the Jahn–Teller distortion and the protrusion of the TM atom, affect the band-gap opening in TM–silicene.

To verify this assumption, the effects of these geometric changes on the band-gap opening were thoroughly investigated. The substitution of an impurity atom instead of a Si atom breaks the symmetry of the two sublattices, which has a great impact on the electronic characteristics of silicene. Furthermore, two other variations in the geometry, mentioned above, also led to the breaking of the symmetry of the two sublattices. First, because of the Jahn–Teller effect, a doped TM atom is displaced from the center of the three nearest Si atoms in Co-, Ni-, and Cu-doped silicene, as shown in Figure 4b. This displacement changes the interatomic distances between the TM and Si atoms, which are correlated with the electronic structure. From this result, the equivalence of two sublattices was broken by the distortion of the Si honeycomb lattice, and more sublattice symmetry breaking was introduced. Second, the protrusion of a TM atom influences the two symmetric sublattices in a different way. In addition to this geometric effect, an electric charge, which stemmed from the charge transfer between the protruding TM atom and the silicene, led to an internal vertical electric field (Table 2). However, the intensity of this vertical electric field is different at the two sublattices, owing to the distinction of the distance from the TM atom to the two sublattices by the buckled height in silicene. Therefore, the electric symmetry of the two sublattices in silicene is broken. Although these protrusions of the TM atom and the charge transfer are also introduced in the cases of Sc, V, Cr, Mn, and Fe doping (Table S1), the vertical electric field in these cases leads to a gap opening that is not at the E_F, but occurs at another energy level, and this gap opening is less important in band-gap engineering. Thus, it is verified that the symmetry breaking in the two sublattices induced by the structural alterations is associated with the band-gap opening.

3. Conclusions

The band-gap opening at the E_F in silicene upon substitution of a 3d TM (from Sc to Zn) atom was studied by using DFT calculations. As a gap opening is introduced by an electric field or metal adsorption, TM doping on silicene also leads to a gap opening. This gap results from the sublattice symmetry breaking through Jahn–Teller distortion and an internal vertical electric field. However, it was discovered from the DFT calculations that only in Ti-, Co-, Ni-, Cu-, and Zn-doped silicene, among the ten types of TM–silicene, was there a significant band gap, which includes the E_F. Ti, Ni, and Zn doping change the substrate to a semiconductor, and Co- and Cu-doped silicene have a half-metallic band gap at E_F. These band-gap openings at E_F could play an essential role in using TM–silicene in nanoelectronic devices, in fields such as quantum electronics, spintronics, and optoelectronics. In particular, Ti-doped silicene is considered to be the most appropriate material for practical applications because of its geometric stability, relatively large direct band gap, and good compatibility with Si-based technology through the absence of distortion in the substrate. In the present paper, the effect of a single 3d TM atom on the electronic structure of a 4×4 silicene supercell is considered. Therefore, more studies about the doping concentration of TM atoms in silicene need to be discussed further.

Acknowledgements

This research was supported by the Basic Science Research Program through the National Research Foundation of Korea (NRF), funded by the Ministry of Education (2013R1A1A2A10064432).

Keywords: band gap · density functional calculations · silicene · substitution · transition metals

[1] X. Lin, J. Ni, *Phys. Rev. B* **2012**, *86*, 075440.
[2] M. Houssa, G. Pourtois, V. Afanasev, A. Stesmans, *Appl. Phys. Lett.* **2010**, *97*, 112106 – 112106.
[3] P. Vogt, P. De Padova, C. Quaresima, J. Avila, E. Frantzeskakis, M. C. Asensio, A. Resta, Bé. Ealet, G. Le Lay, *Phys. Rev. Lett.* **2012**, *108*, 155501.
[4] A. K. Geim, *Science* **2009**, *324*, 1530 – 1534.
[5] A. K. Geim, K. S. Novoselov, *Nat. Mater.* **2007**, *6*, 183 – 191.
[6] Z.-G. Shao, X.-S. Ye, L. Yang, C.-L. Wang, *J. Appl. Phys.* **2013**, *114*, 093712.
[7] C.-C. Liu, W. Feng, Y. Yao, *Phys. Rev. Lett.* **2011**, *107*, 076802.
[8] S. Cahangirov, M. Topsakal, E. Aktürk, H. Şahin, S. Ciraci, *Phys. Rev. Lett.* **2009**, *102*, 236804.
[9] C.-C. Liu, H. Jiang, Y. Yao, *Phys. Rev. B* **2011**, *84*, 195430.
[10] S. Cahangirov, M. Audiffred, P. Tang, A. Iacomino, W. Duan, G. Merino, A. Rubio, *Phys. Rev. B* **2013**, *88*, 035432.
[11] M. Houssa, G. Pourtois, M. Heyns, V. Afanasev, A. Stesmans, *J. Electrochem. Soc.* **2011**, *158*, H107 – H110.
[12] L. Meng, Y. Wang, L. Zhang, S. Du, R. Wu, L. Li, Y. Zhang, G. Li, H. Zhou, W. A. Hofer, H.-J. Gao, *Nano Lett.* **2013**, *13*, 685 – 690.
[13] B. Feng, Z. Ding, S. Meng, Y. Yao, X. He, P. Cheng, L. Chen, K. Wu, *Nano Lett.* **2012**, *12*, 3507 – 3511.
[14] A. Fleurence, R. Friedlein, T. Ozaki, H. Kawai, Y. Wang, Y. Yamada-Takamura, *Phys. Rev. Lett.* **2012**, *108*, 245501.
[15] L. Chen, C.-C. Liu, B. Feng, X. He, P. Cheng, Z. Ding, S. Meng, Y. Yao, K. Wu, *Phys. Rev. Lett.* **2012**, *109*, 056804.
[16] C.-L. Lin, R. Arafune, K. Kawahara, N. Tsukahara, E. Minamitani, Y. Kim, N. Takagi, M. Kawai, *Appl. Phys. Express* **2012**, *5*, 045802.
[17] B. Lalmi, H. Oughaddou, H. Enriquez, A. Kara, Sé. Vizzini, Bé. Ealet, B. Aufray, *Appl. Phys. Lett.* **2010**, *97*, 223109 – 223109.
[18] N. Drummond, V. Zolyomi, V. Fal'Ko, *Phys. Rev. B* **2012**, *85*, 075423.
[19] M. Ezawa, *Phys. Rev. Lett.* **2012**, *109*, 055502.
[20] D. D. Awschalom, M. E. Flatté, *Nat. Phys.* **2007**, *3*, 153 – 159.
[21] I. žutić, J. Fabian, S. D. Sarma, *Rev. Mod. Phys.* **2004**, *76*, 323.
[22] S. Wolf, D. Awschalom, R. Buhrman, J. Daughton, S. Von Molnar, M. Roukes, A. Y. Chtchelkanova, D. Treger, *Science* **2001**, *294*, 1488 – 1495.
[23] W. E. Pickett, J. S. Moodera, *Phys. Today* **2001**, *54*, 39.

[24] J.-H. Park, E. Vescovo, H.-J. Kim, C. Kwon, R. Ramesh, T. Venkatesan, *Nature* **1998**, *392*, 794 – 796.
[25] W. Geng, X. Zhao, W. Zan, H. Liu, X. Yao, *Phys. Chem. Chem. Phys.* **2014**, *16*, 3542 – 3548.
[26] B. Kang, H. Liu, J. Y. Lee, *Phys. Chem. Chem. Phys.* **2014**, *16*, 974 – 980.
[27] P. Nath, D. Sanyal, D. Jana, *Phys. E* **2014**, *56*, 64 – 68.
[28] Z.-Z. Lin, Q. Wei, X. Zhu, *Carbon* **2014**, *66*, 504 – 510.
[29] B. Doumi, A. Tadjer, F. Dahmane, A. Djedid, A. Yakoubi, Y. Barkat, M. O. Kada, A. Sayede, L. Hamada, *J. Supercond. Nov. Magn.* **2014**, *27*, 293 – 300.
[30] C.-L. Lin, R. Arafune, K. Kawahara, M. Kanno, N. Tsukahara, E. Minamitani, Y. Kim, M. Kawai, N. Takagi, *Phys. Rev. Lett.* **2013**, *110*, 076801.
[31] J. Koo, H. J. Hwang, B. Huang, H. Lee, H. Lee, M. Park, Y. Kwon, S.-H. Wei, H. Lee, *J. Phys. Chem. C* **2013**, *117*, 11960 – 11967.
[32] J. Yun, Z. Zhang, T. Yin, *Sci. World J.* **2013**, 541496.
[33] Y. Li, Z. Zhou, P. Shen, Z. Chen, *Acs Nano* **2009**, *3*, 1952 – 1958.
[34] R. Quhe, R. Fei, Q. Liu, J. Zheng, H. Li, C. Xu, Z. Ni, Y. Wang, D. Yu, Z. Gao, J. Lu, *Sci. Rep.* **2012**, *2*, 853.
[35] J. Gao, J. Zhang, H. Liu, Q. Zhang, J. Zhao, *Nanoscale* **2013**, *5*, 9785 – 9792.
[36] V. O. Ozcelik, S. Ciraci, *J. Phys. Chem. C* **2013**, *117*, 26305 – 26315.
[37] X.-T. An, Y.-Y. Zhang, J.-J. Liu, S.-S. Li, *Appl. Phys. Lett.* **2013**, *102*, 043113 – 043113.
[38] H. H. Gürel, V. O. Özçelik, S. Ciraci, *J. Phys. Condens. Matter* **2013**, *25*, 305007.
[39] X.-L. Zhang, L.-F. Liu, W.-M. Liu, *Sci. Rep.* **2013**, *3*, 2908.
[40] Z. Ni, Q. Liu, K. Tang, J. Zheng, J. Zhou, R. Qin, Z. Gao, D. Yu, J. Lu, *Nano Lett.* **2012**, *12*, 113 – 118.
[41] H. Sahin, F. M. Peeters, *Phys. Rev. B* **2013**, *87*, 085423.
[42] G. Kresse, Jü. Furthmüller, *Comput. Mater. Sci.* **1996**, *6*, 15 – 50.
[43] G. Kresse, Jü. Furthmüller, *Phys. Rev. B* **1996**, *54*, 11169.
[44] G. Kresse, Jü. Hafner, *Phys. Rev. B* **1993**, *47*, 558.
[45] J. P. Perdew, K. Burke, M. Ernzerhof, *Phys. Rev. Lett.* **1996**, *77*, 3865.
[46] G. Kresse, D. Joubert, *Phys. Rev. B* **1999**, *59*, 1758.
[47] H. J. Monkhorst, J. D. Pack, *Phys. Rev. B* **1976**, *13*, 5188 – 5192.
[48] G. Makov, M. Payne, *Phys. Rev. B* **1995**, *51*, 4014.
[49] A. Kara, H. Enriquez, A. P. Seitsonen, L. Lew Yan Voon, Sé. Vizzini, B. Aufray, H. Oughaddou, *Surf. Sci. Rep.* **2012**, *67*, 1 – 18.
[50] D. Jose, A. Datta, *Acc. Chem. Res.* **2014**, *47*, 593 – 602.
[51] D. Jose, A. Datta, *J. Phys. Chem. C* **2012**, *116*, 24639 – 24648.
[52] I. B. Bersuker, *Chem. Rev.* **2001**, *101*, 1067 – 1114.
[53] J. Zhang, B. Zhao, Z. Yang, *Phys. Rev. B* **2013**, *88*, 165422.
[54] E. J. Santos, A. Ayuela, D. Sánchez-Portal, *New J. Phys.* **2010**, *12*, 053012.
[55] G. Henkelman, A. Arnaldsson, H. Jónsson, *Comput. Mater. Sci.* **2006**, *36*, 354 – 360.

Received: September 3, 2014
Published online on October 9, 2014